

Spin Dynamics for the t - J Model

Zhongbing Huang² and Shiping Feng^{1,2,3}

¹CCAST (World Laboratory) P. O. Box 8730, Beijing 100080, China

^{2*}Department of Physics, Beijing Normal University, Beijing 100875, China

³National Laboratory of Superconductivity, Academia Sinica, Beijing 100080, China

The spin dynamics at the finite temperature for the t - J model in the underdoped and optimal doped regimes is studied within the fermion-spin theory. It is shown that the dynamical spin structure factor spectrum at the antiferromagnetic wave vector $Q = (\pi, \pi)$ are separated as low- and high-frequency parts, respectively, but the high-frequency part is suppressed in the dynamical susceptibility spectrum $\chi''(Q, \omega)$, while the low-frequency part is the temperature dependent, which are in qualitative agreement with the experiments and numerical simulations.

71.27.+a, 74.72.-h, 76.60.-k

The t - J model provides one of the most interesting and simplest models to study the physics of the doped Mott insulator¹. It was originally introduced as an effective Hamiltonian of the Hubbard model in the strong coupling regime², where the on-site Coulomb repulsion U is very large as compared with the electron hopping energy t , and in this case the electrons become strongly correlated to avoid the double occupancy, i.e., $\sum_{\sigma} C_{i\sigma}^+ C_{i\sigma}^- \leq 1$. The interest in the two-dimensional (2D) t - J model was stimulated by many researchers' suggestion that it contains the relevant physics of the copper oxide superconductors¹.

During the past ten years, consistent experiments picture of the magnetic properties of the copper oxide materials have been emerged^{3,4}: the undoped copper oxide materials are antiferromagnetic Mott insulators, and upon doping with holes in the copper oxide sheets, the antiferromagnetic long-range-order (AFLRO) is replaced by short-range spin correlations, and the dynamic antiferromagnetic correlations persist even into the superconducting state. A series of the neutron-scattering study^{5,6} of the copper oxide materials shows that there is an anomalous temperature dependence of the spin fluctuations near the antiferromagnetic zone center in the underdoped and optimal doped regimes, which has a much larger effect on the spin dynamics and leads to the unusual temperature dependence of the spin-lattice relaxation time. On the theoretical side, the spin dynamics in the underdoped and optimal doped regimes has been studied within the phenomenological model of antiferromagnetic correlated spins⁷, and the framework of the phenomenological marginal Fermi-liquid theory⁸. Moreover, the most reliable results of the spin dynamics have been obtained by the numerical simulations⁹ and high-temperature series expansion¹⁰ based on some strongly correlated models. It is believed that the role played by the magnetism, particularly the nature of spin fluctuations, is the central issue of the copper oxide materials. In this paper, we employ the t - J model to study the spin dynamics of the copper oxide materials in the underdoped and optimal doped regimes within the fermion-spin theory^{11,12}, and show that our theoretical results are qualitative consistent with the experiments⁵ and numer-

ical simulations⁹.

In order to account for the real experiments under the t - J model, the crucial requirement is to impose the electron on-site local constraint for a proper understanding of the physics of the copper oxide materials¹³. For incorporating the local constraint, the fermion-spin theory based on the charge-spin separation has been proposed¹¹. In this approach, the constrained electron operators are decoupled as $C_{i\uparrow} = h_i^+ S_i^-$ and $C_{i\downarrow} = h_i^+ S_i^+$, with the spinless fermion operator h_i keeps track of the charge (holon), while the pseudospin operator S_i keeps track of the spin (spinon). The advantage of the fermion-spin theory is that the electron on-site local constraint for the single occupancy is satisfied even in the mean-field approximation (MFA). Within the fermion-spin theory, the mean-field theory¹² in the underdoped and optimal doped regimes has been developed, where the mean-field order parameters are defined as $\chi = \langle S_i^+ S_{i+\eta}^- \rangle = \langle S_i^- S_{i+\eta}^+ \rangle$, $\chi_z = \langle S_i^z S_{i+\eta}^z \rangle$, $C = (1/Z^2) \sum_{\eta, \eta'} \langle S_{i+\eta}^+ S_{i+\eta'}^- \rangle$, $C_z = (1/Z^2) \sum_{\eta, \eta'} \langle S_{i+\eta}^z S_{i+\eta'}^z \rangle$, and $\phi = \langle h_i^\dagger h_{i+\eta} \rangle$, with $\hat{\eta} = \pm\hat{x}, \pm\hat{y}$, and Z is the number of nearest neighbor sites. This mean-field theory¹² has been applied to study the electron spectrum, electron dispersion, and electron density of state of the copper oxide materials, and the results are in agreement with the experiments and numerical simulations. In the fermion-spin representation, the t - J model is written as $H = H_t + H_J$ with

$$H_t = -t \sum_{i\eta} h_i h_{i+\eta}^\dagger (S_i^+ S_{i+\eta}^- + S_i^- S_{i+\eta}^+) + h.c. + \mu \sum_i h_i^\dagger h_i, \quad (1a)$$

$$H_J = J_{eff} \sum_{i\eta} \left[\frac{1}{2} (S_i^+ S_{i+\eta}^- + S_i^- S_{i+\eta}^+) + S_i^z S_{i+\eta}^z \right], \quad (1b)$$

where $J_{eff} = J[(1 - \delta)^2 - \phi^2]$, and μ is the chemical potential. Based on the Ioffe-Larkin combination rule¹⁴, the charge dynamics of the copper oxide materials in the underdoped and optimal doped regimes has been discussed¹⁵ by considering the charge fluctuations around the mean-field solution. However, the spin fluctuations couple only to spinons and therefore no composition law

is required¹⁴ in discussing the spin dynamics, but the effect of holons still is considered through the holon's order parameter ϕ entering in the spinon propagator. For discussing the spin dynamics, we need to calculate the second-order correction for the spinon by going beyond MFA. The second-order spinon self-energy diagram from the holon pair bubble is shown in Fig. 1. The mean-field spinon Green's functions $D^{(0)}(k, \omega)$ and $D_z^{(0)}(k, \omega)$, and mean-field holon Green's function $g^{(0)}(k, \omega)$ have been given in Ref.¹². Since the spinon operator obey the Pauli algebra, it is needed to map the spinon operator into the CP^1 fermion representation or the spinless-fermion representation in terms of the $2D$ Jordan-Wigner transformation¹⁶ for the formal many particle perturbation expansion. After such formal expansion, the spinon Green's function in the spinon self-energy diagram shown in Fig. 1 is replaced by the mean-field spinon Green's function $D^{(0)}(k, \omega)$, then the second-order spinon self-energy is evaluated as,

$$\begin{aligned} \Sigma_s^{(2)}(k, \omega) = & -(Zt)^2 \frac{1}{N^2} \sum_{pp'} (\gamma_{k-p} + \gamma_{p'+p+k})^2 B_{k+p'} \\ & \times \left(\frac{F_1(k, p, p')}{\omega + \xi_{p+p'} - \xi_p + \omega_{k+p'} + i0^+} \right. \\ & \left. - \frac{F_2(k, p, p')}{\omega + \xi_{p+p'} - \xi_p - \omega_{k+p'} + i0^+} \right), \end{aligned} \quad (2)$$

where $F_1(k, p, p') = n_F(\xi_{p+p'})[1 - n_F(\xi_p)] + [1 + n_B(\omega_{k+p'})][n_F(\xi_p) - n_F(\xi_{p+p'})]$, $F_2(k, p, p') = n_F(\xi_{p+p'})[1 - n_F(\xi_p)] - n_B(\omega_{k+p'})[n_F(\xi_p) - n_F(\xi_{p+p'})]$, $n_F(\xi_k)$ and $n_B(\omega_k)$ are the Fermi and Bose distribution functions, respectively, $\gamma_{\mathbf{k}} = (1/Z) \sum_{\eta} e^{i\mathbf{k} \cdot \hat{\eta}}$, $B_k = Z J_{eff} [(2\epsilon\chi_z + \chi)\gamma_k - (\epsilon\chi + 2\chi_z)]/\omega(k)$, $\epsilon = 1 + 2t\phi/J_{eff}$, and the mean-field holon excitation spectrum ξ_k and mean-field spinon excitation spectrum ω_k are given in Ref.¹². In this case, the full spinon Green's function is obtained as $D^{-1}(k, \omega) = D^{(0)-1}(k, \omega) - \Sigma_s^{(2)}(k, \omega)$.

As manifestation of the spin dynamics, the dynamical spin structure factor $S(k, \omega)$ and dynamical susceptibility $\chi(k, \omega)$ are given as

$$\begin{aligned} S(k, \omega) = & Re \int_0^{\infty} dt e^{i\omega t} \langle S_k^+(t) S_k^-(0) \rangle \\ = & \frac{2\text{Im}D(k, \omega)}{(1 - e^{-\beta\omega})}, \end{aligned} \quad (3)$$

and

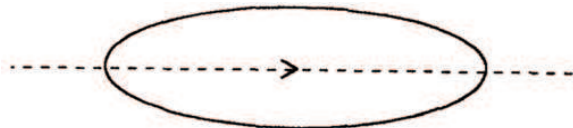


FIG. 1. The spinon's second-order self-energy diagram. The solid and dashed lines correspond to the holon and spinon propagators, respectively.

$$\begin{aligned} \chi''(k, \omega) = & (1 - e^{-\beta\omega}) S(k, \omega) \\ = & 2\text{Im}D(k, \omega), \end{aligned} \quad (4)$$

respectively. Although the detailed magnetic properties depend on the sample preparation method in the experiments as well as the precise value and homogeneity of the oxygen content, the anomalous temperature dependence of the spin fluctuations near the antiferromagnetic wave vector $Q = (\pi, \pi)$ seems common⁵⁻⁷. We have performed the numerical calculation for the dynamical structure factor (3) and dynamical susceptibility (4). The result of the $S(Q, \omega)$ spectra at the doping $\delta = 0.06$ (solid line) and $\delta = 0.15$ (dashed line) with the temperature $T = 0.2J$ are plotted in Fig. 2. It is shown that in the underdoped and optimal doped regimes there are the coexistence of the low- and high-frequency fluctuations in the $S(Q, \omega)$ spectra, the excitations are remark-

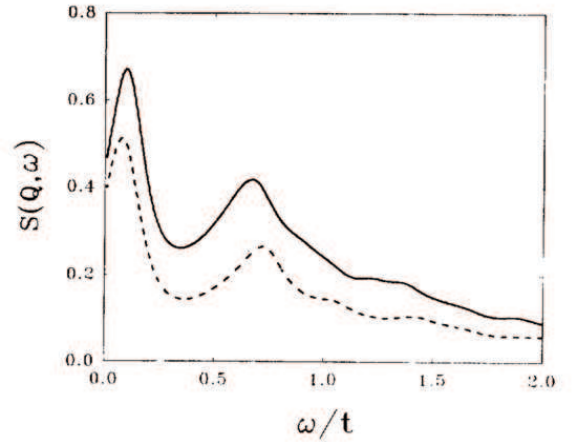


FIG. 2. The dynamical spin structure factor spectra $S(Q, \omega)$ in the temperature $T = 0.2J$ for the doping $\delta = 0.06$ (solid line) and $\delta = 0.15$ (dashed line).

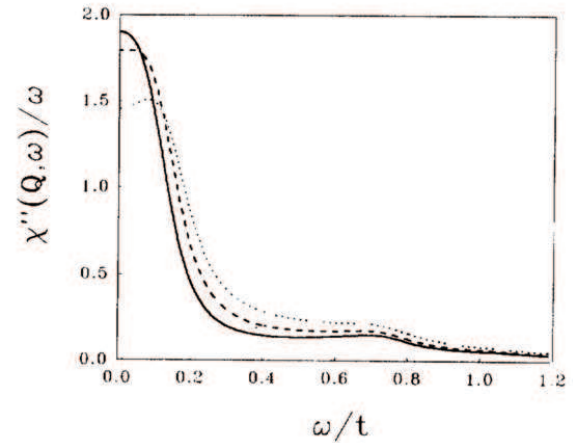


FIG. 3. The dynamical spin susceptibility spectra $\chi''(Q, \omega)/\omega$ at the doping $\delta = 0.15$ for the temperature $T = 0.2J$ (solid line), $T = 0.3J$ (dashed line), and $T = 0.45J$ (dotted line).

ably sharp, and the spectra are changed with dopings, which is consistent with the experiments⁵ and numerical simulation⁹. The low-frequency peak in Q point is due to the antiferromagnetic fluctuations, which will be in existence even in the undoped case, and dominate dynamical susceptibility and the neutron-scattering processes, while the high-frequency peak may come from the contribution of the free-fermion-like component of the systems, which induces the main effect to the large extent the static spin correlation. In correspondence with the $S(Q, \omega)$ spectra, the numerical results of the dynamical susceptibility spectra $\chi''(Q, \omega)$ at the doping $\delta = 0.15$ for the temperature $T = 0.2J$ (solid line), $T = 0.3J$ (dashed line), $T = 0.45J$ (dotted line) are plotted in Fig. 3. Comparing with the Fig. 2, it is shown that although the high-frequency peak is suppressed in the $\chi''(Q, \omega)$ spectra, however, it still is separated from the low-frequency part at the antiferromagnetic wave vector Q . Our results also indicate that the low-frequency peak of the dynamical susceptibility $\chi''(Q, \omega)$ is temperature dependent, while the high-frequency part is almost temperature independent, which are consistent with the experiments⁵ and numerical simulations⁹. The present theoretical results have been used¹⁷ to extract the integrated susceptibility and spin-lattice relaxation time, and the results shown that the integrated susceptibility exhibits the particularly universal behavior as $1/N \sum_k \chi''(k, \omega) \propto \arctan[a_1\omega/T + a_3(\omega/T)^3]$ and the spin-lattice relaxation time is weakly temperature dependent.

In summary, we have studied the spin dynamics of the t - J model in the underdoped and optimal doped regimes within the fermion-spin theory. It is shown that there are two peaks for the dynamical spin structure factor at the antiferromagnetic wave vector Q , but the high-frequency peak is suppressed in the dynamical susceptibility spectra $\chi''(Q, \omega)$, which are qualitative consistent with the experiments and numerical simulations.

ACKNOWLEDGMENTS

This work is supported by the National Science Foundation Grant No. 19474007, and the Trans-Century Training Programme Foundation for the Talents by the State Education Commission of China.

* Mailing address.

¹ P. W. Anderson, *Science* **235**, 1196 (1987); F. C. Zhang and T. M. Rice, *Phys. Rev.* **B37**, 3759 (1988).

² C. Gros, R. Joynt, and T. M. Rice, *Phys. Rev.* **B36**, 381 (1987).

- ³ A. P. Kampf, *Phys. Rep.* **249**, 219 (1994), and references therein.
- ⁴ See, e. g., *High Temperature Superconductivity*, Proc. Los Alamos Symp., 1989, K. S. Bedell *et al.*, eds. (Addison-Wesley, Redwood City, California, 1990).
- ⁵ B. Keimer *et al.*, *Phys. Rev. Lett.* **67**, 1930 (1991); R. J. Birgeneau *et al.*, *Z. Phys.* **B87**, 15 (1992); B. J. Sternlieb *et al.*, *Phys. Rev.* **B47**, 5320 (1993); Matsuda *et al.*, *Phys. Rev.* **B49**, 6958 (1994).
- ⁶ W. O. Putikka *et al.*, *Phys. Rev. Lett.* **73**, 170 (1994); T. Tohyama *et al.*, *Physica* **C215**, 382 (1993); T. Imai *et al.*, *Phys. Rev. Lett.* **70**, 1002 (1993).
- ⁷ A. J. Millis, H. Monien, and D. Pines, *Phys. Rev.* **B42**, 167 (1990); A. J. Millis and H. Monien, *Phys. Rev.* **B45**, 3059 (1992).
- ⁸ C. M. Varma *et al.*, *Phys. Rev. Lett.* **63**, 1996 (1989).
- ⁹ J. Jaklič and P. Prelovšek, *Phys. Rev. Lett.* **74**, 3411 (1995); E. Dagotto, *Rev. Mod. Phys.* **66**, 763 (1994), and references therein.
- ¹⁰ R. R. P. Singh and R. L. Glenister, *Phys. Rev.* **B46**, 11871 (1992); F. C. Alcaraz and R. R. P. Singh, *Phys. Rev.* **B47**, 8298 (1993).
- ¹¹ Shiping Feng, Z. B. Su, and L. Yu, *Phys. Rev.* **B49**, 2368 (1994); *Mod. Phys. Lett.* **B7**, 1013 (1993); Shiping Feng, *Physica* **C232**, 119 (1994).
- ¹² Shiping Feng and Yun Song, *Phys. Rev.* **B55**, 642 (1997).
- ¹³ L. Zhang, J. K. Jain, and V. J. Emery, *Phys. Rev.* **B47**, 3368 (1993); Shiping Feng *et al.*, *Phys. Rev.* **B47**, 15192 (1993).
- ¹⁴ L. B. Ioffe and A. I. Larkin, *Phys. Rev.* **B39**, 8988 (1989); N. Nagaosa and P. A. Lee, *Phys. Rev. Lett.* **64**, 2450 (1990).
- ¹⁵ Shiping Feng and Zhongbing Huang, *Phys. Lett.* **A232**, 293 (1997); Zhongbing Huang and Shiping Feng (unpublished).
- ¹⁶ E. Mele, *Phys. Scr.* **T27**, 82 (1988); E. Fradkin, *Phys. Rev. Lett.* **63**, 322 (1989).
- ¹⁷ Shiping Feng and Zhongbing Huang (unpublished).